

Theory of ion-ion recombination in plasmas

W. L. Morgan

University of California, Lawrence Livermore National Laboratory, Livermore, California 94550

J. N. Bardsley and J. Lin*

Department of Physics and Astronomy, University of Pittsburgh, Pittsburgh, Pennsylvania 15260

B. L. Whitten

University of California, Lawrence Livermore National Laboratory, Livermore, California 94550

(Received 22 March 1982)

Ionic recombination in a dense plasma is studied by the application of molecular dynamics and Monte Carlo simulations and through the development of transport theory. For charge densities exceeding 10^{14} cm^{-3} , the modification of the effective interaction between positive and negative ions leads to a significant reduction in the recombination rate at pressures below 1 atm. At higher pressures the rate is less sensitive to the ion density. The presence of an external field also inhibits the recombination rate. This latter effect may be especially important in rare-gas-halide discharge laser plasmas.

I. INTRODUCTION

There has been a resurgence of interest recently in ion-ion recombination due to the development of excimer lasers. In rare-gas-halide and metal-vapor-halide lasers, recombination of rare gas or metal positive ions and halogen negative ions is the formation mechanism for the upper laser state.¹ Although experimental measurements of ionic recombination rate coefficients have been performed for some molecular ions (see the review by Mahan²), for most ionic species one must rely upon theoretical calculations. The theory of ionic recombination has a long history, which is discussed in the excellent review of the subject by Flannery.³ In brief, Thomson⁴ gave an early theoretical model for ionic recombination at low pressure, while Langevin⁵ predicted mobility limited recombination at high pressures. More recently, theories by Natanson⁶ and by Bates and Flannery⁷ have bridged the region between low and high pressure. The simplicity of the theory has permitted the development of simple scaling laws and universal curves^{8,9} for molecular recombination.

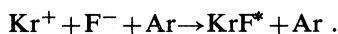
The theoretical work just described has assumed a low ion density where possible collective effects can be ignored. In lasers, however, ion densities may easily exceed 10^{13} cm^{-3} and sometimes even 10^{15} cm^{-3} . In such plasmas, screening of the Coulomb potential between ions by other ions, which should have the effect of slowing down the recombination rate, may be significant. In order to

assess the importance of plasma screening upon ionic recombination, Morgan, Whitten, and Bardsley¹⁰ have performed Monte Carlo calculations of the ionic recombination rate using a Debye-Huckel (DH) screened potential and a simulation procedure developed by Bardsley and Wadehra.¹¹ However, it is assumed in the derivation of the Debye-Huckel potential that there is an equilibrium distribution of charged particles. This is not correct when recombination is occurring, since the flow of oppositely charged particles toward one another modifies the pair-correlation function.¹² The effective potential should instead be obtained from a self-consistent solution of Poisson's equation and the transport equations.¹³ Furthermore, the use of a screening potential neglects the discretization of the charge in the plasma and so introduces some error due to self-screening.

Bates has pointed out another effect that becomes important at such high ion densities. The ions are created at finite separations and one cannot consider recombination as the culmination of the approach of a pair of ions initially at infinite separation. Instead one should introduce a volume source of ions. Bates¹² suggests that at high neutral density the resulting recombination rate must be close to the Langevin-Harper value of $4\pi K e$, where K is the sum of the mobilities of the positive and negative ions.

In this paper we will present an improved transport theory, appropriate at high neutral densities, in which ion-ion recombination is treated in terms of

pair-correlation functions and an effective interionic potential, and will review the Monte Carlo simulations.¹⁰ In both of these approaches the important three-body correlations are treated approximately. The major aim of the paper is to present the results of molecular-dynamics (MD) simulations in which we follow the motion of many interacting ions and so avoid most of the approximations inherent in the other two methods. As in the previous work,¹⁰ the specific reaction studied is



Finally, we will discuss the effect of an external electric field upon the recombination rate.

II. THEORY OF ION-ION RECOMBINATION IN DENSE GASES

In this section we will discuss the theory of recombination in gases in which the neutral density is sufficiently high that diffusion theory can be applied. We will relate the recombination rate to the ionic pair-correlation function and try to avoid the explicit introduction of three-body correlations. Although we will calculate an effective interionic potential, we will take account of the production and recombination of ions and so will not obtain the standard Debye-Huckel form for this potential.

Let $g_+(r)$ be the pair-correlation function (also called the radial-distribution function) for ions of the same charge and $g_-(r)$ be that for oppositely charged ions. Defining the average ion density to be n_i , we write

$$n_{\pm}(r) = n_i g_{\pm}(r) . \quad (1)$$

Then, for example, $n_+(r)$ gives the density of positive ions at a distance r from the position of a given positive ion, and the density of negative ions at the same distance from a known negative ion. Let us further define the associated particle currents to be $\vec{J}_{\pm}(r)$. Thus, at a distance R from a known positive ion, the outward flow of positive ions is given by $\vec{J}_+(R)$, and that of negative ions is $\vec{J}_-(R)$. We assume that the neutral density is sufficiently high that these ionic currents can be calculated by diffusion theory,

$$\vec{J}_{\pm}(r) = -D \vec{\nabla} n_{\pm}(r) \mp K e n_{\pm}(r) \vec{\nabla} \phi(r) . \quad (2)$$

In this equation, D denotes the sum of the diffusion coefficients for the two ion species, K is the sum of the mobilities, and $\phi(r)$ is the average electric potential at a distance r from a positive ion.

Note that the use of Eq. (1) involves several ap-

proximations. The use of a single pair of coefficients, D and K , is correct for the relative motion of oppositely charged ions, but represents an average of the two different values that should be used for the motion of ions of the same charge. This simplification seems worthwhile since we are mainly concerned with the flow of oppositely charged particles, and this approximation avoids the need for the introduction of three correlation coefficients. The use of a single electric potential $\phi(r)$ implies that the average potential experienced by a test charge at a distance r from a given positive (or negative) ion is independent of the sign of the test charge. This is a consequence of our neglect of three-body correlations.

We will assume that recombination can occur only if ions of opposite charge approach to within a separation r_0 , and that w is the probability that any pair of ions whose separation becomes less than r_0 actually do recombine. We will assume that r_0 is sufficiently small that when $r < r_0$ the effective ionic interaction is Coulombic, so that the recombination probability w can be computed using a two-particle Monte Carlo simulation with an unscreened potential.¹¹ On the other hand, r_0 should be large enough that for $r > r_0$ the electric fields are not so strong that diffusion theory becomes invalid. The recombination rate α can then be computed from the net inflow of oppositely charged particles at separation r_0 :

$$\alpha = - \frac{4\pi r^2}{n_i} J_-(r_0) . \quad (3)$$

Using diffusion theory, the inward flow can be written approximately, in terms of the ion density $n_-(r_0)$ and the average relative speed \bar{v} . We find

$$J_-(r_0) = -n_-(r_0) \frac{\bar{v}}{4} w . \quad (4)$$

The electric potential $\phi(r)$ is obtained from the Gauss solution to Poisson's equation. We write

$$\phi(r) = e \int_r^{\infty} \frac{q(r')}{r'^2} dr' , \quad (5)$$

where the screened charge $q(r)$ is given by

$$q(r) = 1 + 4\pi \int_0^r [n_+(r') - n_-(r')] r'^2 dr' . \quad (6)$$

To ensure total charge neutrality we require

$$\int_0^{\infty} [n_+(r') - n_-(r')] r'^2 dr' = -1 , \quad (7)$$

so that

$$q(r) = -4\pi \int_r^{\infty} [n_+(r') - n_-(r')] r'^2 dr' . \quad (8)$$

The particle current $\vec{J}_{\pm}(r)$ must satisfy the continuity equation

$$\vec{\nabla} \cdot \vec{J}_{\pm}(r) = S(r), \quad (9)$$

where $S(r)$ is a volume source term, which is equal to the difference between the rate of creation of ion pairs at a separation r and the rate of disappearance of ion pairs due to recombination of either ion with a third charged particle. We will assume that ion creation occurs homogeneously at a rate sufficient to balance the recombination events. The rate of third-body recombination is proportional to the probability of finding two ions of opposite charge at the same distance r from a reference charge. Thus we write

$$S = \alpha n_i^2 - \alpha n_+(r)n_-(r). \quad (10)$$

Note that

$$S(r) \rightarrow 0 \text{ as } r \rightarrow \infty, \quad (11)$$

provided that

$$n_{\pm}(r) \rightarrow n_i \text{ as } r \rightarrow \infty. \quad (12)$$

This is required if the net production rate is to remain finite when integrated over all space.

Returning to Eq. (2), let us assume that coefficients of mobility and diffusion are connected through the Einstein relation. The outward flow of particles is then given by

$$J_{\pm}(r) = -D \left[\frac{d}{dr} \mp \frac{e^2}{kT} \frac{q(r)}{r^2} \right] n_{\pm}(r), \quad (13)$$

and the continuity equation becomes

$$\begin{aligned} \frac{-D}{r^2} \frac{d}{dr} \left[r^2 \left(\frac{d}{dr} - \frac{e^2}{kT} \frac{q(r)}{r^2} \right) n_{\pm}(r) \right] \\ = \alpha [n_i^2 - n_+(r)n_-(r)], \end{aligned} \quad (14)$$

where $q(r)$ is given, in terms of $n_+(r)$ and $n_-(r)$, by Eq. (6). Hence we have a pair of coupled integro-differential equations, which form a fourth-order nonlinear system.

These equations have been solved numerically, using an iterative procedure, based on the Newton-Raphson algorithm. The outer boundary r_{∞} is assumed to be sufficiently large that the ion densities are uniform and the field is zero, i.e., we require

$$q(r_0) = 0, \quad (15)$$

$$n_-(r_{\infty}) = n_i. \quad (16)$$

The inner boundary is taken to be r_0 . Here we also impose two conditions. First, we assume negligible

screening of each ion for $r \leq r_0$ so that $q(r_0)$ is unity. Second, we assume that the current of oppositely charged particles is given by Eq. (3). If the recombination rate α is specified, there is then a unique solution and the correlation functions can be computed at all distances. By varying α we can study the effect of the inward flow of oppositely charged ions upon the pair-correlation function and screening. This procedure shows that some values of α are unacceptable because, if α is too large, $n_-(r)$ becomes negative in the region around r_0 , and the solution is clearly unphysical. This leads to an upper limit upon the recombination rate that we will call the Townsend limit.¹⁴ This limit can be computed by imposing the further condition

$$n_-(r_0) = 0. \quad (17)$$

In Eq. (4) we expressed the net inward current of oppositely charged ions as the product of the number of incoming ions reaching the separation r_0 , per unit time, and the recombination probability. If the recombination probability w is known, for example from a Monte Carlo simulation or from a detailed microscopic theory such as that of Flannery,¹⁵ and the average speed v can be estimated, then this equation can be used as the final boundary condition. In the limit of very high neutral density, the recombination probability can be taken as unity and the speed v can be assigned its thermal value $(8kT/\pi\mu)^{1/2}$, in which μ is the reduced mass of the two ions. The recombination rate is then close to the Townsend limit.

The standard theory of recombination can be recovered from this theory when the average ionic separation \bar{r}_i satisfies

$$\frac{e^2}{\bar{r}_i} \ll kT. \quad (18)$$

In this limit the potential $\phi(r)$ becomes Coulombic and the source term in the continuity equation small. The Townsend limit is then given by

$$\alpha = \frac{4\pi K e}{1 - \exp(-e^2/r_0 kT)}. \quad (19)$$

For high neutral densities one can choose r_0 so that

$$r_0 \ll \frac{e^2}{kT} \quad (20)$$

and the recombination rate is then close to the Langevin-Harper value $4\pi K e$.

In Sec. V we will apply this theory to the recombination of Kr^+ and F^- in Ar gas, and examine the dependence of the correlation coefficients $g_{\pm}(r)$ and recombination rate upon the average ion density n_i .

III. REVIEW OF THE MONTE CARLO SIMULATIONS

The principles of the study of ionic recombination by Monte Carlo techniques are described in Refs. 10 and 11. The procedure involves two calculations: (1) the calculation, using a Monte Carlo simulation, of the recombination probability w for two ions starting at a distance r_0 apart, with speeds selected from a thermal distribution and interacting through some force law; and (2) the calculation of the flux of ions crossing the surface of the sphere of diameter r_0 from $r > r_0$.

In the calculations reported in Ref. 10, the Debye-Huckel potential was used in both parts of the calculation. The ion flux was calculated using Fick's law [Eq. (2)] but the source term in Eq. (9) was neglected. In the Monte Carlo simulation, the ions describe classical trajectories between collisions with the neutral atoms. Following the Langevin model, the frequency of ion-neutral collisions was taken to independent of velocity and the differential cross section was assumed to be isotropic. The ions are followed until either their relative energy becomes less than $-12kT$, in which case recombination is judged to have occurred, or until their separation becomes greater than r_0 .

When the separation between two ions is less than the average distance between neighboring ions \bar{r}_i , the Debye-Huckel potential may overestimate the screening effects because of the contribution from self-screening. Thus for $r_0 \leq \bar{r}_i$ it may be preferable to ignore the screening effects in step (1) of the Monte Carlo simulation, and to use a Coulomb interaction in the calculation of w .

Figure 1 shows the calculated rate for the recombination of Kr^+ and F^- in Ar at 300 K. The continuous lines show the results obtained previously with a Coulomb potential, and with the Debye-Huckel potential appropriate to ion densities of 10^{13} and 10^{15} cm^{-3} . The value of r_0 used in this calculation was $1000a_0$. For the higher ion density we also show the recombination rate obtained by the hybrid technique described above, in which one uses a Coulomb potential in the calculation of the recombination probability w , and the Debye-Huckel potential in the calculation of the flux of ions with a separation of r_0 . At an ion density of 10^{13} these two methods give almost identical results.

These results show that a significant dependence of the recombination rate on ion density arises because of the effect of screening on the pair-correlation function for $r \geq r_0$. Thus it is important that we examine the behavior of this correlation

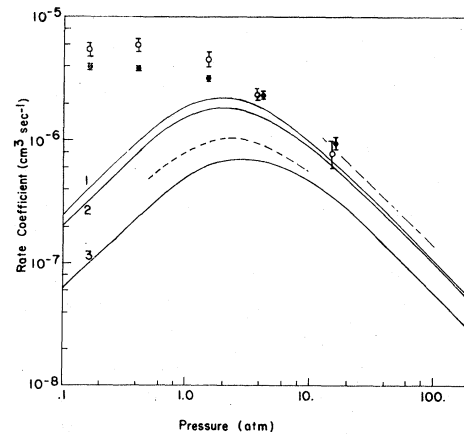


FIG. 1. Recombination-rate coefficient for Kr^+ and F^- in Ar. Solid curves are Monte Carlo calculations from Ref. 10 for ion densities of: (1) 0; (2) 10^{13} cm^{-3} ; (3) 10^{15} cm^{-3} . Dashed curve at intermediate pressure is a Monte Carlo calculation for $n_i = 10^{15}$ using the hybrid technique described in Sec. III of the text. Points labeled with \circ and \bullet are molecular-dynamics absorbing-sphere calculations for $n_i = 10^{13}$ and 10^{15} cm^{-3} rate, respectively. Dashed curve at high pressure is the limit given by Eq. (19).

function more carefully without recourse to the Debye-Huckel approximation. We will do this both by means of a many-body simulation and by applying the transport theory described in Sec. II.

IV. MANY-BODY SIMULATIONS BY THE MOLECULAR-DYNAMICS METHOD

A comprehensive review of the method of molecular dynamics (MD) has been written by Kushick and Berne.¹⁶ Briefly, the classical equations of motion of a number of particles in a unit cell with periodic boundary conditions are integrated in time. Nearest images¹⁷ of the particles are used in the calculation of interparticle forces. For the integration of equations of motion for the system of ions we have used the algorithm of Scofield¹⁸:

$$r(t+dt) = r(t) + v(t)dt + [4a(t) - a(t-dt)]dt^2/6, \quad (21a)$$

$$v(t+dt) = v(t) + [2a(t+dt) + 5a(t) - a(t-dt)]dt/6. \quad (21b)$$

The ions are assumed to collide with the neutral atoms with the Langevin constant collision frequency mentioned previously in Sec. III. Because of this we need only follow the ions in the simulation and not the neutral particles. This simulation represents

a constant (T, V, N) canonical ensemble in that the neutral atoms function as a thermal reservoir which maintains a constant temperature. Additionally, as ions disappear from the volume due to recombination, new ion pairs are created in the unit cell with uniform spatial distribution and random thermal velocities. Hence the ion density is held constant in time.

During the course of the MD simulation we calculate a variety of quantities. The radial distribution functions $g_+(r)$ and $g_-(r)$ are obtained directly by counting the number of ion pairs with separation close to r . Diffusion coefficients for the positive and negative ions in the neutral gas can be computed from the mean-square displacement of the ions as a function of time.¹⁹ If there is an applied electric field, we also calculate a drift velocity in the direction of the field.

In our molecular-dynamics simulation of ionic recombination we have used 100 ions (50 of each type) in a cubic cell with sides of length $32\,314a_0$ and $6962a_0$ corresponding to ion densities of $n_i = 10^{13}$ and 10^{15} cm^{-3} , respectively. A typical time step used in this simulation is

$$10^4 \tau_0 \leq \Delta t \leq 5 \times 10^5 \tau_0,$$

where $\tau_0 = 2.42 \times 10^{-17}$ sec is the atomic unit of time. The time step used in these calculations is determined by the ion-neutral collision frequency. This is, typically, at least several orders of magnitude faster than the frequency of recombination. Because recombination is a relatively infrequent event, a great number of time steps are required for any reasonable statistical accuracy, with low ion density and high pressure representing the most severe case. In the calculations described below, for example, the number of time steps used ranges from 6×10^4 to 2×10^5 for $n_i = 10^{13}$ cm^{-3} .

If two unlike ions approach to within a distance r_0 of each other, we allow one of four things to happen, depending on what we desire to study during the simulation. The four options are (i) the ions can rebound as elastic hard spheres, (ii) the ions can recombine, (iii) we can perform the Monte Carlo simulation^{10,11} using the Coulomb force between the ions to determine whether they recombine or not, and (iv) two ions are said to recombine when their relative energy is less than some E_{crit} . Option (i) allows us to investigate the radial distribution functions and transport coefficients in a plasma in the absence of recombination. Option (ii) is the absorbing-sphere model representing the maximum recombination rate and allowing us to study the effects of recombination on the $g(r)$ and the diffusion

coefficients. A partially absorbing sphere can also be used. Options three and four are the most realistic simulations. Option (iii) is most useful in the intermediate-pressure range where the recombination rate is large and where a large time step can be used. Option (iv) can only be used at high pressures where the collisional mean-free path is small enough that even close ions do not reach speeds very much greater than thermal. This constraint is required by the accuracy of the rather simple integration algorithm.

V. APPLICATION TO $\text{Kr}^+ \text{F}^-$ RECOMBINATION IN ARGON

Let us first consider the results obtained by the molecular-dynamics method with option (ii), the absorbing-sphere model, since this option involves the smallest statistical uncertainties. The recombination rates computed for ion densities of 10^{13} and 10^{15} cm^{-3} , $r_0 = 500a_0$, are shown in Fig. 1. At low pressure, the rate is clearly lower at the higher ion density. At higher pressures, the difference between the rates at the two densities is much less, and both results are close to the Langevin rate, as predicted by Bates.¹²

Further insight into these results can be obtained from the pair-correlation functions $g_+(r)$ and $g_-(r)$. Figure 2 shows the results at the relatively low pressure of 0.04 atm. The dashed curves (C) and the continuous curves labeled by DH 13 and DH 15 represent equilibrium distributions appropriate to Coulomb interactions and Debye-Huckel potentials, respectively. The absence of long-range correlation in DH 15 is evident. The correlation function for oppositely charged ions $g_-(r)$ is greater than unity, whereas $g_+(r)$ is between zero and one. The circles and squares represent MD calculations of $g_-(r)$ for elastic spheres. The agreement with the Debye-Huckel theory is good. The curves labeled MD 13 and MD 15 are the MD results for ion densities of 10^{13} and 10^{15} , respectively. The inflow of oppositely charged particles leads to a considerable reduction in $g_-(r)$ in the neighborhood of $r = r_0$. We still see, however, significant screening effects.

At low pressures, the probability w that recombination occurs within the sphere $r < r_0$ is much less than one, and a partially absorbing sphere would be a more reasonable model. The correlation functions will then lie between the limits represented by the DH and MD curves in Fig. 2, and the effect of screening will be important.

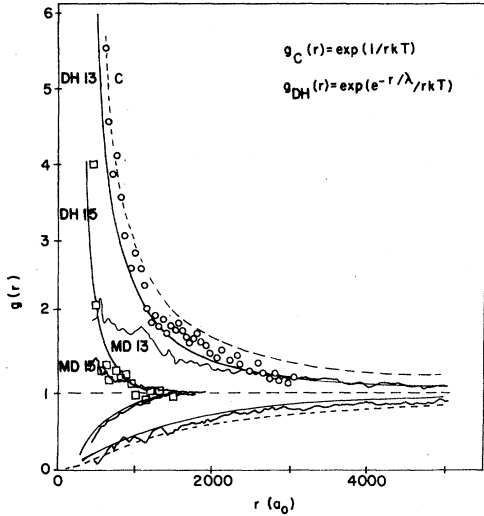


FIG. 2. Pair-correlation functions $g_-(r)$ and $g_+(r)$ (greater than and less than 1, respectively) at $P=0.04$ atm. Dashed curve (C) is the Coulomb function $g_C(r)$ and the smooth solid curves DH 13 and DH 15 are the Debye-Huckel functions $g_{DH}(r)$ for $n_i=10^{13}$ and 10^{15} cm^{-3} , respectively. Points \circ and \square are MD calculations of $g_-(r)$ for elastic spheres. Curves labeled MD 13 and MD 15 are MD calculations of $g_{\pm}(r)$ for absorbing spheres with $r_0=500a_0$.

At high pressure, the effect of the recombination upon the correlation function $g_-(r)$ is even more dramatic. As shown in Fig. 3(a), which corresponds to a pressure of 16 atm, $g_-(r)$ is everywhere below 1, becoming smaller as $r \rightarrow r_0$. The effect of raising the ion density from 10^{13} to 10^{15} is to move $g_-(r)$ towards unity, thus increasing the correlation function in the neighborhood of r_0 . This may lead to an

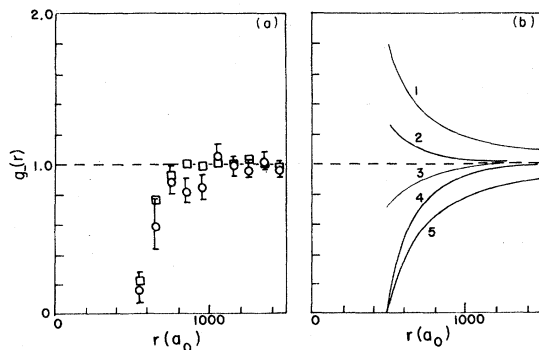


FIG. 3. (a) MD calculations of $g_-(r)$ for $P=16$ atm and $n_i=10^{13}$ cm^{-3} (\circ) and 10^{15} cm^{-3} (\square). (b) $g_-(r)$ from transport theory for (1) $n_i=10^{13}$ cm^{-3} , $\alpha=6.0 \times 10^{-7}$ $\text{cm}^3 \text{sec}^{-1}$; (2) $n_i=10^{15}$, $\alpha=6.0 \times 10^{-7}$; (3) $n_i=10^{15}$, $\alpha=8.25 \times 10^{-7}$; (4) $n_i=10^{15}$, $\alpha=1.125 \times 10^{-6}$; (5) $n_i=10^{13}$, $\alpha=8.25 \times 10^{-7}$.

increase in the recombination rate. Although the results, plotted in Fig. 1, are consistent with such an increase, the statistical uncertainty is too large for us to be sure of this effect.

These high-pressure results can be compared with the predictions of the transport theory described in Sec. II. For each of the two values of the ion density we have computed the correlation functions $g_-(r)$ and $g_+(r)$ for several values of the recombination rate. The Townsend boundary condition $n(r_0)=0$ leads to recombination rates of 8.25×10^{-7} $\text{cm}^3 \text{sec}^{-1}$ when $n_i=10^{13}$ cm^{-3} and 1.125×10^{-6} $\text{cm}^3 \text{sec}^{-1}$ when $n_i=10^{15}$ cm^{-3} . These values are slightly higher than the results obtained in the molecular-dynamics calculation. The difference between the two Townsend limits can be understood in terms of the corresponding correlation functions, $g_-(r)$, which are shown in Fig. 3(b). In both calculations $g_-(r)$ is zero at $500a_0$ and increases towards unity as r approaches the average distance between neighboring ions. Since this limit is reached more rapidly at the higher ion density, the slope (dg_-/dr) is larger near $r=r_0$ and the diffusive flow is enhanced.

If the inflow of oppositely charged particles is reduced, for example, by setting $\alpha=6 \times 10^{-7}$ $\text{cm}^3 \text{sec}^{-1}$ in the solution of the transport equations, then the correlation coefficients revert to the form that we found at lower pressure, with $g_-(r)$ being greater than 1 and $g_+(r)$ being less than 1. Changing the ion density from 10^{13} to 10^{15} cm^{-3} then leads to a reduction in $g_-(r)$ and an increase in $g_+(r)$. When $\alpha=7.0 \times 10^{-7}$ $\text{cm}^3 \text{sec}^{-1}$, $g_-(r)$ is close to 1 for all values of r for both values of the ion density.

In order to study the pressure dependence of the recombination rate, we have performed molecular dynamics calculations for $n_i=10^{13}$ cm^{-3} using option (iii), with Monte Carlo simulation of close encounters between oppositely charged ions. In Fig. 4 the results are compared with our old Monte Carlo calculations. At pressures above 1 atm the new results are slightly lower. We have also performed calculations at 16 and 60 atm for $n_i=10^{15}$ cm^{-3} using option (iv). These results confirm that the rate is not strongly sensitive to ion density at such high pressures.

VI. RECOMBINATION IN A DISCHARGE

As mentioned in Sec. I we can simulate recombination in a discharge using molecular dynamics. We performed this calculation for conditions typi-

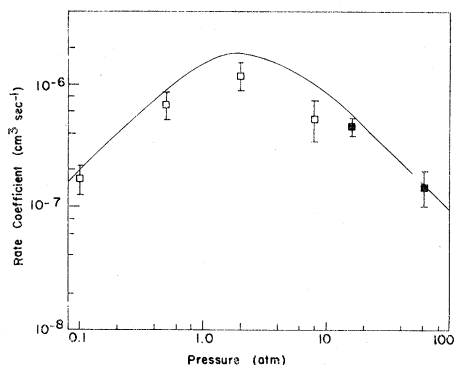


FIG. 4. $\text{Kr}^+ + \text{F}^-$ Ar recombination-rate coefficient. Solid line is curve (2) from Fig. 1. Points \square are MD calculations for $n_i = 10^{13} \text{ cm}^{-3}$ using MD option (iii) (see Sec. IV of text). Points \square are MD calculations for $n_i = 10^{15} \text{ cm}^{-3}$ using MD option (iv).

cal of a krypton-fluoride discharge laser.²⁰ The problem then is recombination of Kr^+ and F^- in helium. The pressure-dependent recombination rate for zero field is shown in Fig. 5. These calculations were made with the Monte Carlo option (iii). Owing to the small mass of He, α peaks at higher pressure than it did with an argon buffer. The field-dependent rate is shown in Fig. 6. Here α is plotted versus E/N , where N is the total number density. These calculations were performed using the molecular-dynamics option (iv) for a pressure of 3 atm and an ion density of $n_i = 10^{15} \text{ cm}^{-3}$. There is a significant reduction in the recombination rate with the application of an electric field.

Bardsley and Wadehra¹¹ have demonstrated for the field-free case that increases in the gas temperature lead to significant reductions in the recombination rate, and Bates⁸ has shown that scaling laws can be derived for simple collision models such as

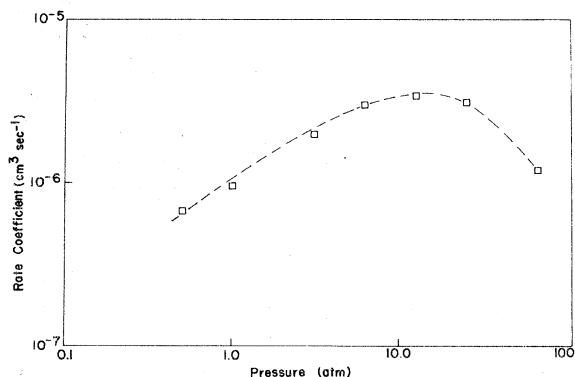


FIG. 5. Rate coefficient for recombination of $\text{Kr}^+ + \text{F}^-$ in He for $E/N = 0$ and $n_i = 10^{15} \text{ cm}^{-3}$.

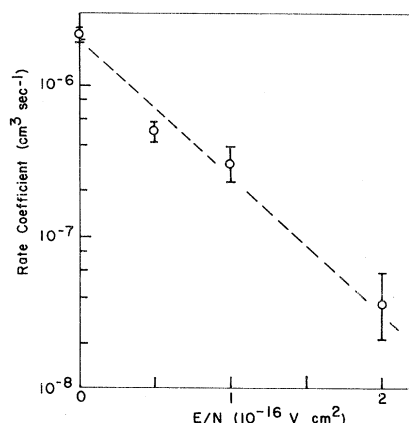


FIG. 6. $\text{Kr}^+ + \text{F}^-$ He recombination-rate coefficient vs discharge E/N for $P = 3 \text{ atm}$ and $n_i = 10^{15} \text{ cm}^{-3}$.

that used here. The presence of the field raises the kinetic energy of the ions well above that of the neutrals. For E/N equal to 20 Td, where 1 Td = 10^{-7} V cm^2 the drift velocities of the F^- and Kr^+ ions are approximately 1.4×10^5 and $1.0 \times 10^5 \text{ cm sec}^{-1}$, respectively, suggesting an effective ion temperature of $\sim 3000 \text{ K}$. The existence of two widely differing temperatures leads to difficulties in the application of such scaling laws, but a significant inhibition of recombination is expected.

An alternative way to view this phenomenon is through the effect of the field on the interionic interaction, which becomes

$$V_{\text{eff}}(r) = -\frac{e^2}{r} - e\vec{E} \cdot \vec{r}.$$

At a pressure of 3 atm, with E/N equal to 20 Td, this potential has a saddle point with $r = 500a_0$ and $V_{\text{eff}} = -0.11 \text{ eV}$. Thus recombination is likely only when a collision of one of the ions with a neutral gas molecule reduces the relative energy to below this value, which is approximately $-4kT$, at a time when the ionic separation is less than $500a_0$.

VII. SUMMARY

We have studied two modifications of the traditional theory of ion-ion recombination which may be necessary in the analysis of the gas discharges in powerful rare-gas-halide lasers. We have demonstrated that, for ion densities over 10^{14} cm^{-3} and neutral densities below 10^{19} cm^{-3} , the recombination rate is reduced due to screening of the interionic interactions, as predicted by the Debye-Huckel theory. For high neutral densities, at which the rate is controlled by the ionic mobility, the Debye-

Huckel theory is inappropriate, as suggested by Bates. We have also studied the effect of the finite separation of the ions at the time when ions are created, by assuming a uniform source of new ions to replace those that disappear through recombination.

The molecular-dynamics method has been used to study the effect of an external electric field upon the recombination process. The resulting increase in the average kinetic energy of the ions and the modification of the effective interionic potential lead to a significant reduction in the recombination rate, even at relatively modest field strengths.

ACKNOWLEDGMENTS

The authors wish to thank Dr. F. J. Rogers and Professor Sir D. R. Bates for helpful conversations and Dr. H. E. DeWitt for suggesting the application of molecular-dynamics methods to this problem. This work was performed under the auspices of the Department of Energy at the Lawrence Livermore National Laboratory under Contract No. W-7405-Eng-48. The work of J.N.B. and J.L. was supported by the National Science Foundation under Grant No. 81-05074.

*Present address: Inter System, Inc., 7630 Little River Turnpike, Annandale, Va. 22003.

¹M. R. Flannery, *Int. J. Quantum Chem. Symp.* **13**, 501 (1979).

²B. H. Mahan, *Adv. Chem. Phys.* **23**, 1 (1973).

³M. R. Flannery, *Atomic Processes and Applications*, edited by P. G. Burke and B. L. Moiseiwitsch (North-Holland, Amsterdam, 1976).

⁴J. J. Thomson, *Philos. Mag.* **47**, 337 (1924).

⁵P. Langevin, *Ann. Chim. Phys.* **29**, 433 (1903).

⁶G. L. Natanson, *Zh. Tekh. Fiz.* **29**, 1373 (1959) [*Sov. Phys.—Tech. Phys.* **4**, 1263 (1959)].

⁷D. R. Bates and M. R. Flannery, *Proc. R. Soc. London, Ser. A* **69**, 910 (1968).

⁸D. R. Bates, *J. Phys. B* **13**, L623 (1980).

⁹D. R. Bates, *Chem. Phys. Lett.* **75**, 409 (1980).

¹⁰W. L. Morgan, B. L. Whitten, and J. N. Bardsley, *Phys. Rev. Lett.* **45**, 2021 (1980).

¹¹J. N. Bardsley and J. M. Wadehra, *Chem. Phys. Lett.* **72**, 477 (1980).

¹²D. R. Bates, *J. Phys. B* **14**, L115 (1981).

¹³M. R. Flannery, *Chem. Phys. Lett.* **80**, 541 (1981).

¹⁴J. S. Townsend, *Electricity in Gases* (Clarendon, Oxford, 1915), pp. 208–220.

¹⁵M. R. Flannery, *Philos. Trans. R. Soc. London, Ser. A* **304**, 447 (1982).

¹⁶J. Kushick and B. J. Berne, in *Statistical Mechanics, Part B*, edited by B. H. Berne (Plenum, New York, 1977).

¹⁷W. W. Wood and F. R. Parker, *J. Chem. Phys.* **22**, 720 (1957).

¹⁸P. Scofield, *Comput. Phys. Commun.* **5**, 17 (1973).

¹⁹E. Helfand, *Phys. Rev.* **119**, 1 (1960).

²⁰A. E. Greene and C. A. Brau, *J. Quantum Electron.* **QE-14**, 951 (1978).